Spectrochimica Acta Part A: Molecular and Biomolecular Spectroscopy 249 (2021) 119297

Contents lists available at ScienceDirect

Spectrochimica Acta Part A: Molecular and Biomolecular Spectroscopy

journal homepage: www.elsevier.com/locate/saa

Synthesis and photophysical properties of ditrifluoroacetoxyboron complexes with curcumin analogues

Lian Cai, Hengyi Du, Dan Wang, Heng Lyu, Dunjia Wang *

College of Chemistry and Chemical Engineering, Hubei Key Laboratory of Pollutant Analysis and Reuse Technology, Hubei Normal University, Huangshi 435002, China

HIGHLIGHTS

- Synthesis of ditrifluoroacetoxyboron complexes with curcumin analogues.
- Solvatochromic effect of boron complexes in different solvents.
- Photophysical behaviors of boron complexes in solution, solid state and PMMA films.

GRAPHICAL ABSTRACT

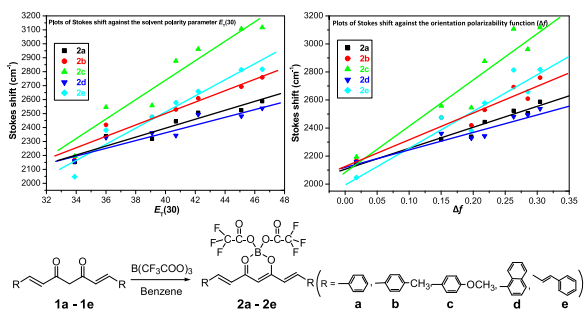

ARTICLE INFO

Article history:
Received 24 August 2020
Received in revised form 25 November 2020
Accepted 29 November 2020
Available online 6 December 2020

Keywords:
Ditrifluoroacetoxyboron complex
Curcumins
Photophysical behaviors
Solvatochromic effect

ABSTRACT

A new class of ditrifluoroacetoxyboron complexes were designed and synthesized by chelation reaction of curcumins with boron trifluoroacetate. Their photophysical behaviors were studied in different solvents, powder state and PMMA polymer films. The results indicated that these complexes revealed a green to yellow emission at 486–595 nm in solution or PMMA films and an orange to red emission at 598–710 nm in powder state. Especially, complex **2c** displayed the strongest emission intensity, the highest quantum yield in solution and the longest fluorescence lifetime in powder state in these complexes. In addtion, the emission bathochromic shifts of these complexes as a function of the solvent polarity parameter $E_T(30)$ were investigated by Lippert–Mataga approximation. It was observed that these complexes exhibited the higher values of the dipole moment difference ($\Delta\mu$) between the ground and excited states, which implied an intense intramolecular charge transfer characteristics and a noticeable emission solvatochromic effect.

1. Introduction

Curcumin (1,7-bis(4-hydroxy-3-methoxyphenyl)-1,6-hepta diene-3,5-diones) is a natural α,β-unsaturated β-diketone compound and possesses good biological and pharmacological properties [1]. During the past two decades, many curcumin analogues (curcuminoids) have been synthesized and their biological activities have been investigated by chemists and biologists [2–5]. Meanwhile, these curcuminoids have good chelation with many metal ions, which were assigned to the presence of the β-diketone in their molecules [6–8], and display good optical and electrical behaviors, which were due to their symmetric structure and highly π-electron delocalized system [9–11]. Up to now, only limited difluoroboron complexes with curcuminoids were prepared and their photophysical and photochemical properties were also investigated in detail [12–15]. The difluoroboron complexes of curcuminoids exhibited the high molar absorption coefficients, strong fluorescence emission, high quantum yields, and second-order nonlinear properties and could be used as fluorescent probes,

* Corresponding author.
E-mail address: dunjiawang@163.com (D. Wang).

https://doi.org/10.1016/j.saa.2020.119297
1386-1425/

chemical sensors and photoluminescent materials [15–18]. Recently, several new diacetoxyboron complexes with curcumin derivatives were reported by our group and their photophysical and solvatochromic properties were also investigated [19]. As a continuation of our work, we designed and synthesized some novel ditrifluoroacetoxyboron complexes with curcumin analogues by replacing C–H bonds of acetoxy groups with C–F bonds to improve their luminescent behaviors because the high-energy oscillators of C–H bonds in molecules can result in the lower photoluminescent properties [20,21]. In addition, the structures of ditrifluoroacetoxyboron complexes were identified and their solvatochromic fluorescent behaviors were investigated in solution, powders and PMMA films in detail.

2. Experimental

2.1. Materials and methods

All reagents and solvents were analytically pure and purchased from commercial suppliers (Sun Chemical Technology or J&K Scientific Ltd.). UV–vis absorption spectra were recorded on a Hitachi U-3010 spectrophotometer. FT-IR spectra were measured on a Nicolet FTIR 5700 spectrophotometer from KBr disks. NMR (^{1}H and ^{13}C) spectra were carried out on a Bruker Avance III™ 300 MHz NMR spectrometer in $CDCl_3$ solution. ESI–MS spectra were obtained with a Finnigan LCQ Advantage Max spectrometer. Emission spectra were measured with a Varian Cary Eclipse fluorescence spectrometer and Quantum yields (Φ) were determined by the standard method using quinine sulfate in 0.1 M sulfuric acid (Φ_s = 0.55, λ_{ex} = 366 nm) as a standard [22]. Fluorescence lifetimes were measured with an Edinburgh FS5 spectrofluorometer by the time-correlated single-proton counting (Instrument response function, IRF = 150 ps, picoseconds pulsed diode laser EPL-450, λ_{ex} = 450 nm). Elemental analyses were performed with a Perkin–Elmer 2400CHN elemental analyzer. Melting points were determined on Beijing Tech X-4 digital melting-point apparatus.

2.2. Synthesis of curcumin analogues (**1a**–**1e**)

The curcumin analogues (**1a**–**1e**) were synthesized by condensation reaction of the aromatic aldehydes with acetylacetone according to our publication [19].

2.3. Synthesis of ditrifluoroacetoxyboron complexes (**2a–2e**)

Boric acid (0.09 g, 1.5 mmol) was added to 15 mL of benzene solution containing trifluoroacetic anhydride (1.3 mL, 9.0 mmol). The mixture was heated to 50 °C and stirred for 1 h to obtain a pink solution of boron trifluoroacetate. The curcumin analogues **1a–1e** (0.5 mmol) were dissolved in 15 mL of benzene and heated to 50 °C, then the above pink solution of boron trifluoroacetate (1.5 mmol) in benzene was added dropwise over 1 h. The mixture was kept stirring for 5 h at 50 °C and the purplish-red solids were formed after cooling to room temperature. The solids were filtered off and recrystallized from chloroform to give ditrifluoroacetoxyboron complexes (**2a–2e**).

Ditrifluoroacetoxyboron 1,7-diphenylhepta-1,6-diene-3,5-dionate (***2a***): Orange powder, yield 62%, m.p. 205–206 °C; IR (KBr): ν 1780 (s), 1603 (s), 1579 (s), 1553 (s), 1495 (m), 1390 (s), 1351 (s), 1220 (s), 1162 (s), 1059 (s), 998 (s), 826 (m), 733 (m) cm^{-1}; ^{1}H NMR (300 MHz, $CDCl_3$): δ 8.02 (d, 2H, *J* = 15.6 Hz, C=C—H), 7.65 (d, 4H, *J* = 6.2 Hz, Ar—H), 7.50–7.45 (m, 6H, Ar—H), 6.79 (d, 2H, *J* = 15.7 Hz, C=C—H), 6.33 (s, 1H, enol C=C—H) ppm; ^{13}C NMR (75 MHz, $CDCl_3$): δ 179.4, 157.3 (q, *J* = 41.7 Hz), 149.1, 133.7, 132.5, 129.5, 129.1, 119.8, 114.1 (q, *J* = 282.6 Hz), 103.5 ppm; ESI–MS *m*/*z*: 534.83 [M+Na]$^+$; Anal. calcd. for $C_{23}H_{15}BF_6O_6$: C 53.94, H 2.95; found C 54.21, H 2.92.

Ditrifluoroacetoxyboron 1,7-di-p-tolylhepta-1,6-diene-3,5-dionate (***2b***): Orange powder, yield 64%, m.p. 231–232 °C; IR (KBr): ν 1784 (s), 1601 (s), 1549 (s), 1501 (s), 1398 (s), 1353 (s), 1220 (s), 1159 (s), 1057 (s), 1020 (m), 976 (m), 821 (m), 746 (m) cm^{-1}; ^{1}H NMR (300 MHz, $CDCl_3$): δ 7.96 (d, 2H, *J* = 15.5 Hz, C=C—H), 7.51 (d, 4H, *J* = 7.7 Hz, Ar—H), 7.23 (d, 4H, *J* = 7.8 Hz, Ar—H), 6.72 (d, 2H, *J* = 15.5 Hz, C=C—H), 6.28 (s, 1H, enol C=C—H), 2.41 (s, 6H, Ar—CH_3) ppm; ^{13}C NMR (75 MHz, $CDCl_3$): δ 178.9, 157.2 (q, *J* = 41.4 Hz), 148.9, 143.6, 131.2, 130.1, 129.6, 118.8, 114.2 (q, *J* = 282.3 Hz), 103.2, 21.8 ppm; ESI–MS *m*/*z*: 562.67 [M+Na]$^+$; Anal. calcd. for $C_{25}H_{19}BF_6O_6$: C 55.58, H 3.54; found C 55.86, H 3.57.

Ditrifluoroacetoxyboron 1,7-Bis(4-methoxyphenyl)hepta-1,6-diene-3,5-dionate (***2c***): Purple powder, yield 67%, m.p. 236–237 °C; IR (KBr): ν 1779 (s), 1599 (s), 1547 (s), 1490 (s), 1397 (s), 1351 (s), 1261 (s), 1216 (s), 1157 (s), 1057 (s), 1023 (s), 974 (m), 828 (s), 746 (m) cm^{-1}; ^{1}H NMR (300 MHz, $CDCl_3$): δ 7.94 (d, 2H, *J* = 15.4 Hz, C=C—H), 7.58 (d, 4H, *J* = 8.5 Hz, Ar—H), 6.94 (d, 4H, *J* = 8.6 Hz, Ar—H), 6.61 (d, 2H, *J* = 15.5 Hz, C=C—H), 6.21 (s, 1H, enol C=C—H), 3.88 (s, 6H, OCH_3) ppm; ^{13}C NMR (75 MHz, $CDCl_3$): δ 178.3, 157.1 (q, *J* = 41.2 Hz), 157.8, 143.7, 130.5, 126.7, 118.2, 115.1, 113.9 (q, *J* = 282.1 Hz), 102.9, 56.6 ppm; ESI–MS *m*/*z*: 594.70 [M + Na]$^+$; Anal. calcd. for $C_{25}H_{19}BF_6O_8$: C 52.48, H 3.35; found C 52.17, H 3.39.

Ditrifluoroacetoxyboron 1,7-Di(naphthalen-1-yl)hepta-1,6-diene-3,5-dionate (***2d***): Purple powder, yield 78%, m.p. 218–219 °C; IR (KBr): ν 1778 (s), 1596 (s), 1572 (s), 1500 (s), 1408 (s), 1356 (s), 1220 (s), 1158 (s), 1046 (s), 956 (m), 828 (m), 718 (m) cm^{-1}; ^{1}H NMR (300 MHz, $CDCl_3$): δ 8.11 (d, 2H, *J* = 15.2 Hz, C=C—H), 7.60 (d, 2H, *J* = 5.0 Hz, Ar—H), 7.49–7.36 (m, 6H, Ar—H), 7.24–7.14 (m, 6H, Ar—H), 6.51 (d, 2H, *J* = 15.2 Hz, C=C—H), 6.19 (s, 1H, enol C=C—H) ppm; ^{13}C NMR (75 MHz, $CDCl_3$): δ 177.9, 157.2 (q, *J* = 42.1 Hz), 147.8, 142.8, 140.1, 139.7, 135.3, 134.8, 132.9, 132.6, 129.3, 129.0, 128.6, 120.1, 114.1 (q, *J* = 282.8 Hz), 103.3 ppm; ESI–MS *m*/*z*: 634.91 [M+Na]$^+$; Anal. calcd. for $C_{31}H_{19}BF_6O_6$: C 60.81, H 3.13; found C 61.16, H 3.18.

Ditrifluoroacetoxyboron 1,11-Diphenyl-undeca-1,3,8,10-tetraene-5,7-dionate (***2e***): Purple powder, yield 72%, m.p. 227–228 °C; IR (KBr): ν 1783 (s), 1586 (s), 1530 (s), 1399 (s), 1351 (s), 1215 (s), 1149 (s), 1053 (s), 1002 (s), 752 (m), 685 (m) cm^{-1}; ^{1}H NMR (300 MHz, $CDCl_3$): δ 7.79 (d, 2H, *J* = 14.7 Hz, C=C—H), 7.54–7.51 (m, 4H, Ar—H), 7.41–7.39 (m, 6H, Ar—H), 7.19 (d, 2H, *J* = 15.4 Hz, C=C—H), 6.98 (dd, 2H, *J* = 15.3, 11.3 Hz, C=C—H), 6.30 (d, 2H, *J* = 14.7 Hz, C=C—H), 6.12 (s, 1H, enol C=C—H) ppm; ^{13}C NMR (75 MHz, $CDCl_3$): δ 178.4, 157.3 (q, *J* = 41.8 Hz), 146.9, 144.5, 136.1, 130.2, 129.3, 128.2, 127.7, 125.3, 114.2 (q, *J* = 282.5 Hz), 103.2 ppm; EI–MS *m*/*z*: 586.68 [M+Na]$^+$; Anal. calcd. for $C_{27}H_{19}BF_6O_6$: C 57.47, H 3.39; found C 57.73, H 3.35.

3. Results and discussion

3.1. Chemistry

The synthesis of ditrifluoroacetoxyboron complexes with curcumin analogues was depicted in Scheme 1. Firstly, the curcumin analogues (**1a**–**1e**) were synthesized by condensation of acetylacetone with the aromatic aldehydes according to our previous paper [19]. Secondly, ditrifluoroacetoxyboron complexes with curcumin analogues (**2a–2e**) were obtained by the chelation reaction with boron trifluoroacetate in benzene. These reaction products were recrystallized from chloroform to give the pure ditrifluoroacetoxyboron complexes and their structures were confirmed by IR, ^{1}H NMR, ^{13}C NMR, ESI–MS spectroscopy and elemental analysis.

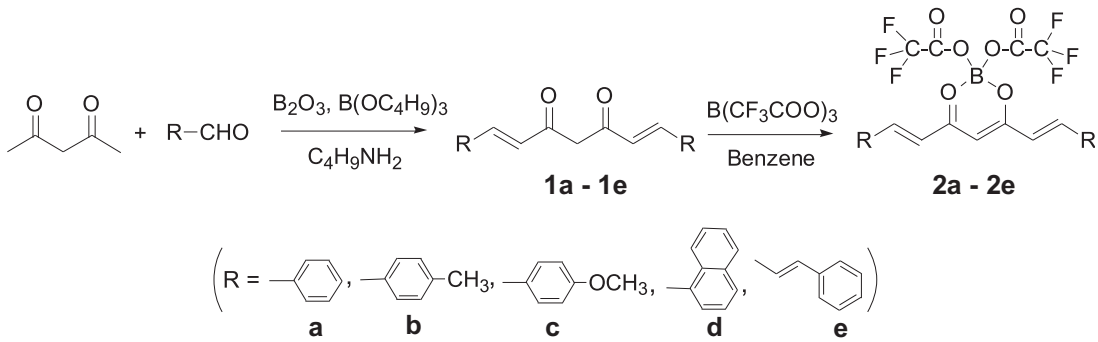

Scheme 1. Synthetic routes of ditrifluoroacetoxyboron complexes **2a–2e.**

In ^{1}H NMR spectra, the chemical shifts at δ = 16.10–15.86 ppm of curcumin analogues [18], which was assigned to the protons of O—H in their keto-enol tautomerism, disappeared completely in those of ditrifluoroacetoxyboron complexes (**2a–2e**). The chemical shifts at δ = 5.96–5.70 ppm in curcumin analogues [19], which was attributed to the protons of enolic C=C—H in their keto-enol tautomerism, moved to the lower field (δ = 6.33–6.12 ppm) in ditrifluoroacetoxyboron complexes. It was probably because of the strong electron-withdrawing effect in six-membered chelate ring by the trifluoroacetoxy moieties. However, chemical shifts of other protons have no large changes. In the IR spectra, the new and strong bands in the range of 1784–1778 cm^{-1} appeared in ditrifluoroacetoxyboron complexes which were the characteristic of the C=O for the trifluoroacetoxy moieties. In these complexes, the C=O and enolic C=C stretching vibrations of the curcumin ligands were red-shifted from 1631–1630 cm^{-1} and 1600–1588 cm^{-1} [19] to 1603–1586 cm^{-1} and 1579–1530 cm^{-1}, respectively, which was because of the formation of six-membered chelate ring containing C=O···B and C=C—O—B bands. The strong infrared bands in the range of 1356–1351 cm^{-1} and 1059–1046 cm^{-1} were assigned to the B—O stretching vibrations. Meanwhile, the strong absorption bands at 1220–1215 cm^{-1} and 1162–1149 cm^{-1} were caused by the C—F stretching modes of trifluoroacetoxy moieties.

3.2. Absorption and fluorescence properties

The absorption and fluorescence spectra in different polar solvents could provide more information about the orientation of ground and excited states in the molecule, so the UV–vis absorption and fluorescence spectra of ditrifluoroacetoxyboron complexes (**2a–2e**) were measured in different polar solvents (the physical properties [23] and polarity parameters [24] of these solvents were presented in Table 1). The normalized absorption spectra of these complexes in different solvents were shown in Fig. 1 and their normalized fluorescence spectra were illustrated in Fig. 2.

The photophysical data of ditrifluoroacetoxyboron complexes, such as the absorption and emission maxima, the Stokes shift and quantum yield in different polar solvents were summarized in Table 2. It was obvious from Table 2 that there was a small alteration of their absorption band position as the polarity of the solvents varied from toluene to DMSO. This phenomenon was similar to that previously reported for diacetoxyboron complexes with curcumin derivatives [19] and it suggested that the transition process from the ground state to the Frank-Condon excited state was similar in different solvents [25]. However, their fluorescence emission of these complexes exhibited remarkable solvatochromic behavior in different solvents (Fig. 2 and Table 2). It turned out that their emission maxima revealed 14–34 nm bathochromic shifts and 378–923 cm^{-1} Stokes shift values and gradually moved toward longer wavelength with increasing solvent polarity. For example, the complex **2c** displayed 38 nm bathochromic shifts in emission peaks from 544 nm in toluene to 578 nm in DMSO and its fluorescence emission from green to orange could be observed in different solvents under UV illumination. These results implied that the emission maxima of ditrifluoroacetoxyboron complexes were dependent upon solvents in contrast to their absorption maxima. The large emission bathochromic shifts in different solvents might result from the intermolecular charge transfer process bringing about more effective reorganization of electronic density in the excited state [26]. This suggested a significant difference between the ground and excited state charge distribution in these complexes [27].

The fluorescence quantum yields of complexes (**2a**–**2e**) in different solvents were determined by taking quinine sulfate (Φ_s = 0.55) as a reference. From Table 2, it was found that these ditrifluoroacetoxyboron complexes exhibited the higher quantum yields in comparison with previously published diacetoxyboron complexes [18] in solution, which was due to the replacement of C–H bonds with C—F bonds. It was probably because of nonradiative deactivation of the energy of excited state resulting from their interaction with high-energy oscillators C—H groups. Meanwhile, it could be seen that complexes **2a**–**2e** displayed the higher fluorescence quantum yields in weak polar solvents and revealed the lower quantum yields in strong polar solvents, which indicated

Table 1
The physical properties and polarity parameters of different polar solvents.

Solvents	Toluene	THF	$CHCl_3$	CH_2Cl_2	Acetone	CH_3CN	DMSO
ε[a]	2.43	7.47	4.89	9.02	21.36	35.94	46.71
n[b]	1.497	1.406	1.446	1.424	1.359	1.344	1.479
$E_T(30)$[c]	33.9	36.0	39.1	40.7	42.2	46.5	45.1
Δf[d]	0.0177	0.1972	0.1503	0.2179	0.2853	0.3046	0.2632

[a] The solvent dielectric constant.
[b] The solvent refractive index.
[c] Reichardt empirical polarity parameters.
[d] The orientation polarizability ($\Delta f = \frac{\varepsilon-1}{2\varepsilon+1} - \frac{n^2-1}{2n^2+1}$).

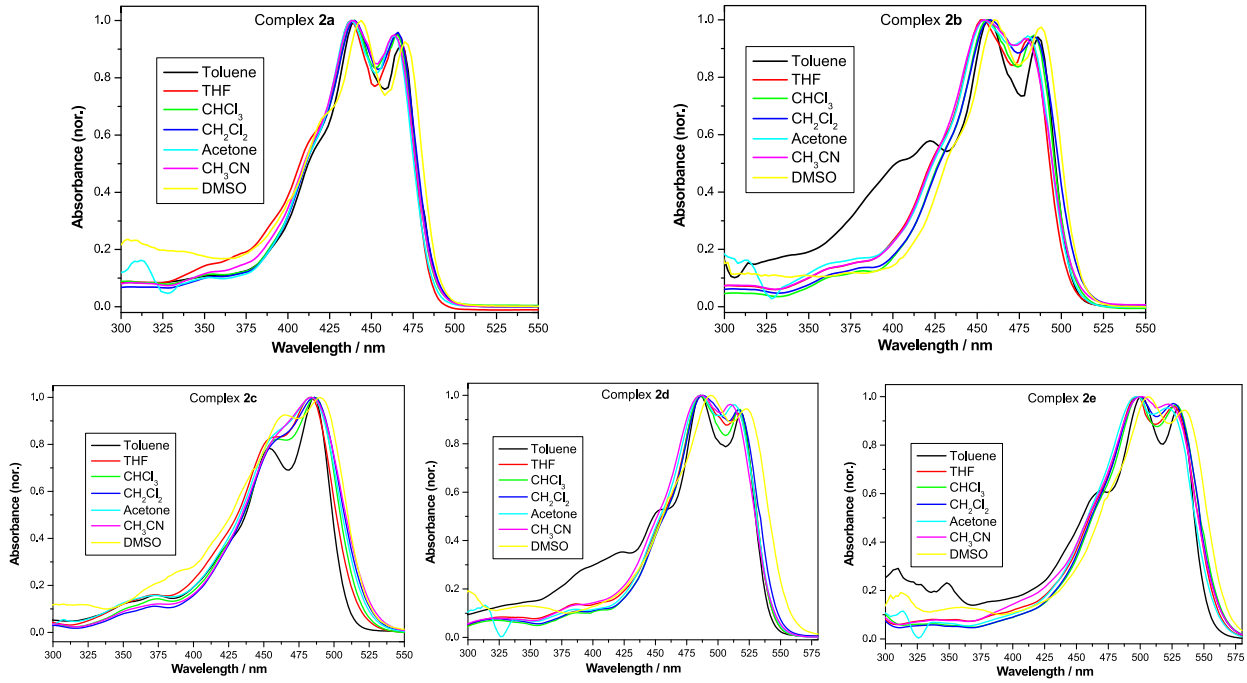

Fig. 1. Normalized UV–vis spectra of complexes 2a–2e in different solvents (1.0×10^{-5} mol·L^{-1}).

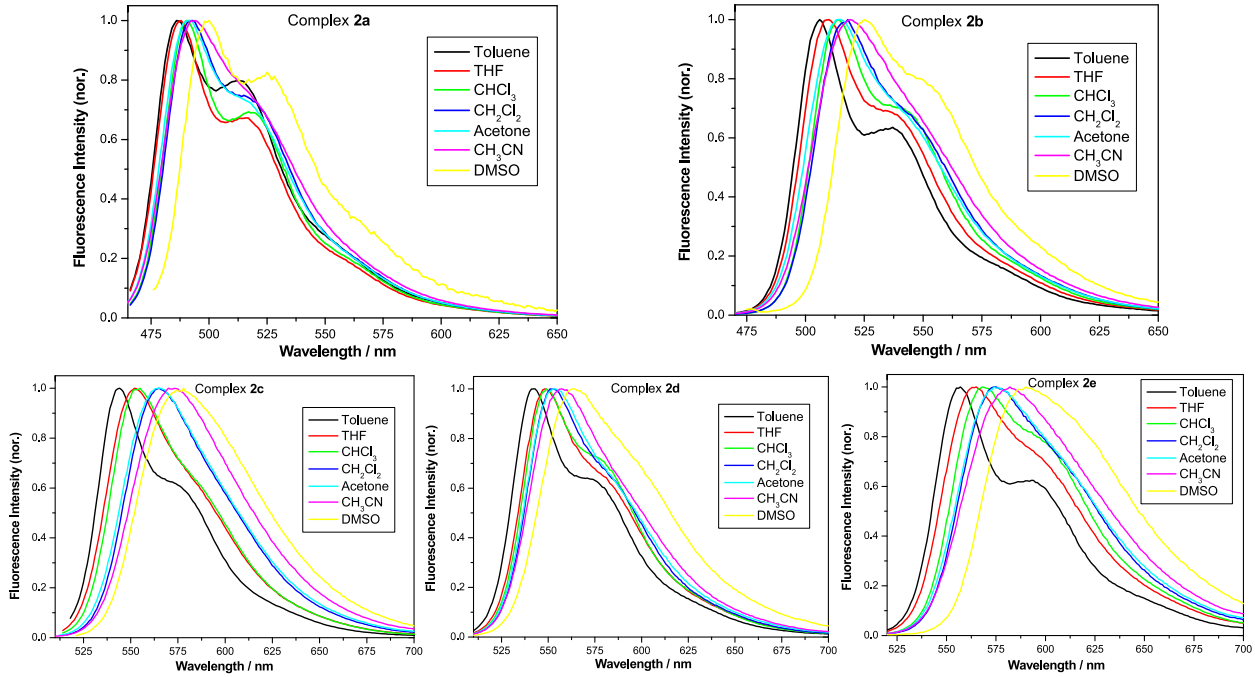

Fig. 2. Normalized emission spectra of complexes 2a–2e in different solvents (1.0×10^{-5} mol·L^{-1}).

that their fluorescence quantum yields were decreased further as the solvent polarity increased [28]. Therefore, a simple explanation might be that the nonradiative decay process was enhanced with increasing the solvent polarity [29]. Additionally, complex **2c** showed the highest fluorescence quantum yield in solution among these complexes, which was attributed to the introduction of the stronger electron-donating methoxyl groups in the chelating system.

In order to understand the solvatochromic effect induced by different polar solvents, the Stokes shifts ($\Delta\nu = \nu_{abs} - \nu_{flu}$) are plotted as a function of the solvent polarity parameter $E_T(30)$ [24], which is an empirical and commonly used method of solvents polarity to analyze solvatochromism. As presented in Figs. 3 and S1–S5, complexes **2a**–**2e** displayed overall increase of Stokes shifts with increasing the solvent polarity. And the relationship between Stokes shifts and $E_T(30)$ exhibited relatively good linear

Table 2
Photophysical data of complexes **2a**–**2e** in different solvents.

Complexes	Solvents	λ_{abc} (nm)	log ε_{max}	λ_{em} (nm)	$\Delta\nu_{stokes}$ (cm^{-1})	Φ_u
2a	Toluene	440	4.72	486	2151	0.76
	THF	438	4.75	488	2339	0.74
	$CHCl_3$	440	4.69	490	2319	0.69
	CH_2Cl_2	440	4.71	493	2443	0.65
	Acetone	438	4.75	492	2506	0.63
	CH_3CN	438	4.72	494	2588	0.62
	DMSO	444	4.81	500	2523	0.59
2b	Toluene	456	4.75	506	2167	0.92
	THF	454	4.77	510	2419	0.81
	$CHCl_3$	456	4.72	514	2475	0.75
	CH_2Cl_2	458	4.73	518	2529	0.70
	Acetone	454	4.74	515	2609	0.73
	CH_3CN	454	4.80	519	2759	0.68
	DMSO	460	4.82	525	2692	0.63
2c	Toluene	486	4.78	544	2194	0.99
	THF	484	4.76	552	2545	0.98
	$CHCl_3$	486	4.73	555	2558	0.95
	CH_2Cl_2	486	4.75	565	2877	0.96
	Acetone	484	4.79	565	2962	0.92
	CH_3CN	484	4.81	570	3117	0.89
	DMSO	490	4.85	578	3107	0.85
2d	Toluene	486	4.65	543	2160	0.86
	THF	486	4.67	548	2328	0.78
	$CHCl_3$	486	4.71	549	2361	0.74
	CH_2Cl_2	488	4.78	551	2343	0.66
	Acetone	486	4.75	553	2493	0.61
	CH_3CN	488	4.76	557	2538	0.53
	DMSO	494	4.73	563	2481	0.42
2e	Toluene	500	4.79	557	2047	0.79
	THF	498	4.78	565	2381	0.63
	$CHCl_3$	498	4.81	568	2475	0.51
	CH_2Cl_2	500	4.80	574	2578	0.48
	Acetone	498	4.85	574	2659	0.45
	CH_3CN	500	4.87	582	2818	0.39
	DMSO	506	4.91	590	2814	0.41

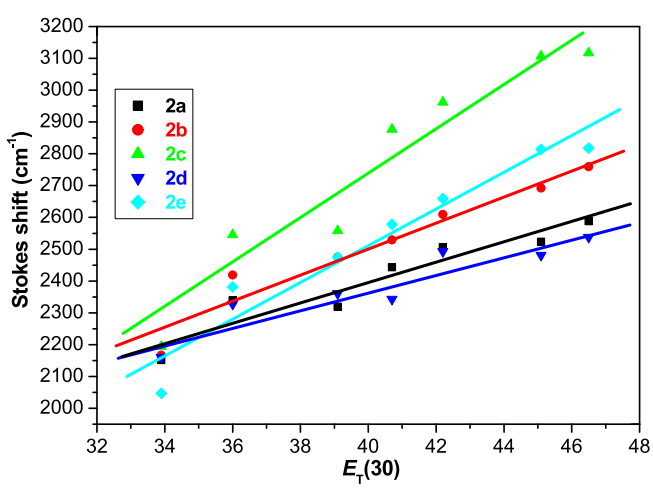

Fig. 3. Plots of Stokes shift against the solvent polarity parameter $E_T(30)$ of complexes **2a**–**2e**.

correlations with the coefficients r = 0.93–0.98, which implied the stronger dependence of fluorescence emission on the different polar solvents.

To gain quantitative insight, the Lippert–Mataga equation (Eq. (1)) [30] can be used to calculate the difference in dipole moments between the excited and ground states ($\Delta\mu$) from the slope of a plot of the Stokes shift ($\Delta\nu$) versus Δf:

$$\Delta\nu = \nu_{abs} - \nu_{flu} = \frac{2\Delta\mu^2}{hca^3}\Delta f + \text{constant} \quad (1)$$

The Δf orientation polarizability is defined as follows (Eq. (2)):

$$\Delta f = \frac{\varepsilon - 1}{2\varepsilon + 1} - \frac{n^2 - 1}{2n^2 + 1} \quad (2)$$

where $\Delta\nu$ is the Stokes shift (in cm^{-1}), ν_{abs} and ν_{flu} are the absorption and emission maxima, respectively, h is the Planck's constant (6.626×10^{-34} Js^{-1}), c is the speed of light (2.998×10^{10} cms^{-1}), ε and n are the dielectric constant and refractive index of corresponding solvent, respectively. In addition, a is the cavity radius, which can be estimated using Van der Waal's volume by Edward's atomic increment method (Eq. (3)) [31,32].

$$a = \left(\frac{3M}{4N\pi d}\right)^{1/3} \quad (3)$$

where M is the molecular weight of the solute, N is Avogadro's number (6.022×10^{23} mol^{-1}), and d is an assumed molecular density of 1 g/cm^3. According to Eq. (3), the cavity radii (a) of complexes **2a–2e** can be calculated as 5.88, 5.98, 6.10, 6.24 and 6.07 Å, respectively.

The Lippert–Mataga plots of complexes **2a–2e** in seven solvents were presented in Figs. 4 and S6–S10. It was found that their correlation coefficient values were 0.94–0.98, indicating a good linearity for these plots. The positive slope implied that the excited state of these complexes was more polarizable than the ground state [33]. Meanwhile, the dipole moment differences between the ground and excited states ($\Delta\mu$) of complexes **2a–2e** were calculated as 17.35, 19.54, 27.33, 17.41 and 24.03 D (debye), respectively, according to the slope of these lines from the Lippert–Mataga equation. The higher values of the dipole moment differences ($\Delta\mu$) indicated the existence of more relaxed excited state, which might be due to intramolecular charge transfer induced by

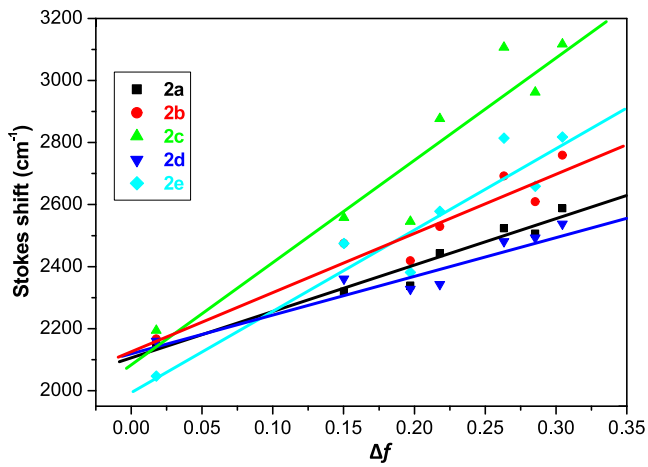

Fig. 4. Plots of Stokes shift against the orientation polarizability function (Δ*f*) of complexes **2a**–**2e**.

the solvent [34]. In particularly, complex **2c** displayed the highest $\Delta\mu$ values in these complexes, suggesting a strong intramolecular charge transfer characteristics and a pronounced emission solvatochromic effect.

3.3. Solid state fluorescence properties

To get a deeper insight into the photophysical properties of these ditrifluoro- acetoxyboron complexes, the solid state emission of powdered complexes **2a–2e** were also investigated at room temperature. From Fig. 5 and Table 3, these complexes exhibited the orange to red emission at 598–710 nm in powders. It was found that the emission maxima of complexes **2a–2e** in powders were strongly red-shifted 76–153 nm compared with those of the corresponding complexes in solution, which was probably due to the intermolecular interactions in solid state [35,36]. Obviously, the complex **2c** exhibited the stronger emission intensity and larger bathochromic effect in solid state, which was assigned to the stronger electron-donating and larger π-conjugated aromatic groups in the boron-chelating system. However, complexes **2d** and **2e** displayed much weaker emission intensities in solid state, which was because of the poor coplanarity on the chelating system resulting from the introduction of naphthyl or cinnamenyl groups

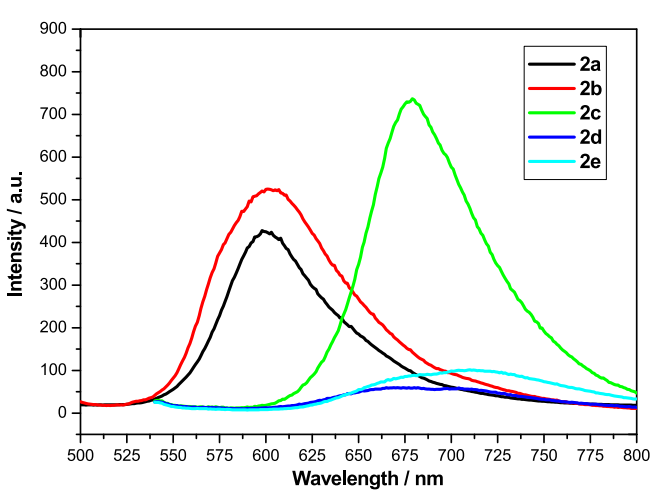

Fig. 5. Emission spectra for complexes **2a**–**2e** in solid powder state at room temperature.

for molecules. In addition, the emission maxima of these complexes showed a remarkable red-shift in comparison with those of diacetoxyboron complexes [19], which was probably due to the electron-withdrawing trifluoromethyl moieties caused by the stronger push–pull π-conjugated system.

Meanwhile, the fluorescence lifetime (τ) of complexes **2a**–**2e** were measured in solid powder state by time-correlated single-photon counting method (TCSPC) and the fluorescence lifetime curves are presented in Fig. 6. Their decay curves were fitted with the software DAS6 to give the fluorescence lifetime values (τ) and the data are listed in Table 3. These complexes revealed only first order progression decay having a single lifetime component with a good χ^2 value of lesser than 1.2. It was found that the complex **2c** displayed the longest fluorescence lifetime value (τ = 19.07 n s), indicating that the introduction of 4-methoxyphenyl group would obviously delay its fluorescence relaxation rate. This is probably because of forming the better push–pull π-conjugated structure in its molecule. However, the complex **2e** revealed the shortest lifetime value (τ = 1.37 ns) in these complexes, which was due to the good rotation of cinnamenyl group in its molecule resulting in accelerating the fluorescence relaxation rate. Their fluorescence lifetime values (τ) decreased in the sequence, **2c** > **2b** > **2d** > **2a** > **2e**.

3.4. Fluorescence properties of pmma@(2a–2e) polymer films

Polymethyl methacrylate (PMMA) exhibited the better mechanical and optical properties that aided its application in optical devices. Therefore, the photophysical behavior of these complexes was further investigated in the PMMA polymer films. These pmma@(**2a**–**2e**) polymer films were prepared by doping with 5 wt% complexes into amorphous PMMA using chloroform as solvent. The prepared pmma@(**2a**–**2e**) polymer films were characterized by FT-IR spectroscopy and presented in Fig. 7. From Fig. 7, the characteristic IR absorption of the PMMA film was at 1723 cm^{-1} (s, $\nu_{C=O}$), 1437 cm^{-1} (s, δ_{CH3}) and 1144 cm^{-1} (s, ν_{C-O}) and IR spectra of pmma@(**2a**–**2e**) polymer films were similar to that of the PMMA film. However, pmma@(**2a**–**2e**) polymer films revealed several new weak absorption peaks at 1782–1776 cm^{-1}, assignable to the C=O stretching vibrations for the trifluoroacetoxy moieties, 1628–1613 cm^{-1} and 1573–1544 cm^{-1}, owing to the C=O and enolic C=C stretching vibrations of the curcumins, and 1067–1057 cm^{-1}, due to the B—O stretching vibrations. It turned out that these complexes had been doped into PMMA films.

The fluorescence behaviors of pmma@(**2a**–**2e**) polymer films were also investigated by using the fluorescence spectrometer (Fig. 8 and Table 3). In pmma@(**2a**–**2e**) polymer films, their emission maxima of exhibited some degree of red-shift in comparison with those of corresponded complexes in solution, which was probably assignable to the less degrees of the conformational freedom in their PMMA films. Like the powder state, the pmma@**3c** film also displayed the strongest emission intensity in these PMMA films. Additionally, the fluorescence lifetimes of pmma@(**2a**–**2e**) polymer films were determined with Edinburgh FS5 spectrofluorometer and their decay curves were listed in Fig. 9. The decay curves were fitted with a DAS6 software to obtain the fluorescence lifetime (τ) and the results were summarized in Table 3. It was observed that the pmma@**2c** film displayed the first order progression decay having a single lifetime component and other PMMA films for complexes revealed the second order progression decay, leading to two component lifetimes [37]. From Table 3, the pmma@**2c** film showed the longest fluorescence lifetime value (τ = 2.47 ns) in these polymer films, which was in agreement with result in powder state. However, their fluorescence lifetime values (τ) in polymer films were much shorter than those for complexes in powder state, which was probably because of the strong interac-

Table 3
Fluorescence data of complexes **2a**–**2e** in powdered state and PMMA polymer film.

Complexes	Powdered state			PMMA polymer film			
	λ_{ex} (nm)	λ_{em} (nm)	τ_1 (ns)	λ_{ex} (nm)	λ_{em} (nm)	τ_1 (ns)	τ_2 (ns)
2a	480	598	3.21	458	508	0.85	7.51
2b	483	601	6.42	470	536	1.36	8.89
2c	516	679	19.07	481	575	2.47	–
2d	535	682	5.73	481	595	1.03	7.27
2e	543	710	1.37	475	586	1.22	10.44

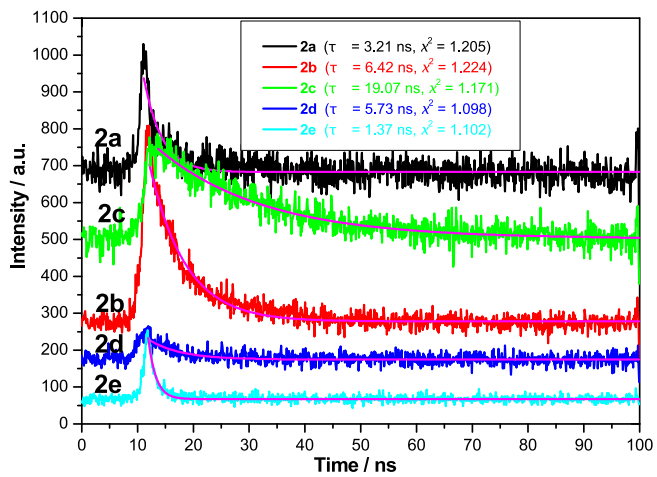

Fig. 6. Fluorescence decay curves of complexes **2a**–**2e** in solid powder state, monitored at 598, 601, 679, 682 and 710 nm, respectively.

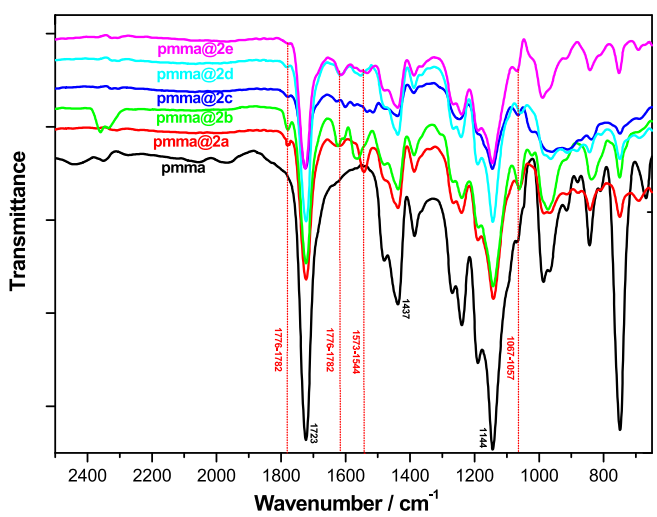

Fig. 7. FT-IR spectra of PMMA film and pmma@(2a–2e) polymer films.

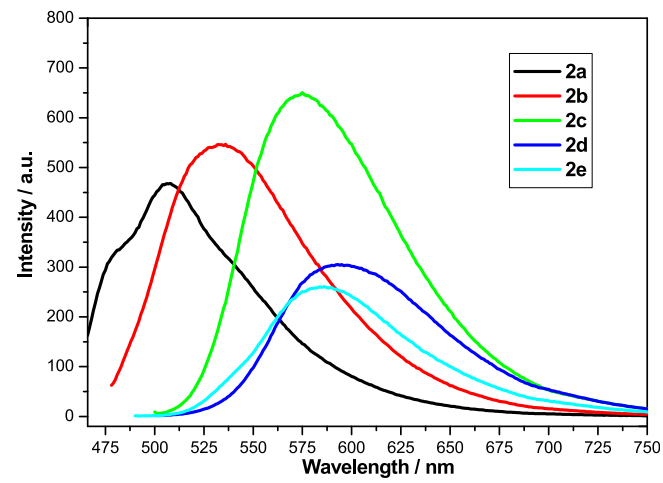

Fig. 8. Emission spectra of pmma@(**2a**–**2e**) polymer films at room temperature.

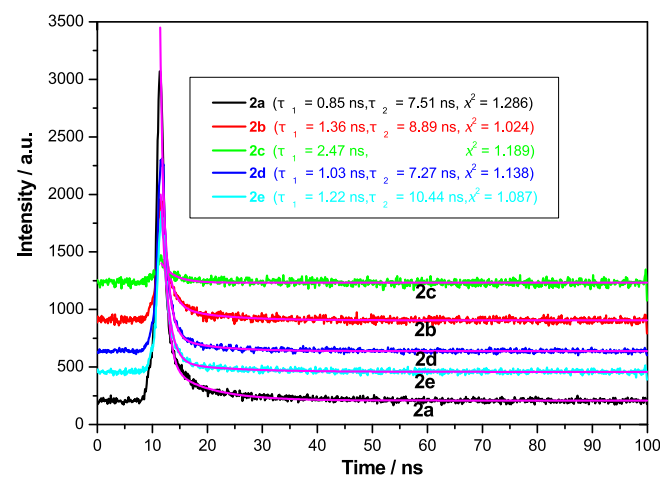

Fig. 9. Fluorescence decay curves of pmma@(**2a**–**2e**) polymer films, monitored at 508, 536, 575, 595 and 586 nm, respectively.

tion between these complexes and PMMA medium resulting in the increase of non-radiative relaxation.

4. Conclusions

In summary, five novel ditrifluoroacetoxyboron complexes with curcumin analogues were synthesized and their structures were confirmed by using FT-IR, ^{1}H NMR, ^{13}C NMR, MS and elemental analysis. Their fluorescence behaviors in solution, powder state and PMMA polymer films were investigated by fluorescence spectroscopy in detail. It was found that these complexes displayed a green to yellow fluorescence in solution or PMMA films, and emitted an orange to red fluorescence in powder state. In particular, complex **2c** exhibited the stronger emission intensity, much higher fluorescence quantum yield (Φ_u = 0.99) in solution and longer fluorescence lifetime value (τ = 19.07 ns) in powder state among these complexes. Meanwhile, the solvatochromic behaviors of these complexes were investigated in different polar solvents by using the solvent polarity parameter approach and Lippert–Mataga plot. The results indicated that these complexes revealed the obvious emission bathochromic shifts with increasing solvent polarity and the high values of the dipole moment difference ($\Delta\mu$). It suggested that the excited state of these complexes were more polarizable than the ground state and their excited state dipole moment were much increased, which was probably assignable to the

intramolecular charge transfer induced by the solvent. In short, this study provided a new design of boron complex for the fluorophore as a promising candidate for photochemistry materials.

CRediT authorship contribution statement

Lian Cai: Conceptualization, Methodology, Investigation, Formal analysis, Validation, Software, Writing - original draft, Writing - review & editing. **Hengyi Du:** Validation, Formal analysis, Software, Writing - original draft, Writing - review & editing. **Dan Wang:** Methodology, Validation, Formal analysis, Writing - review & editing. **Heng Lyu:** Resources, Data curation, Writing - review & editing. **Dunjia Wang:** Conceptualization, Software, Supervision, Data curation, Writing - original draft, Writing - review & editing.

Declaration of Competing Interest

The authors declare that they have no known competing financial interests or personal relationships that could have appeared to influence the work reported in this paper.

Acknowledgment

This work was supported by National Natural Science Foundation of China (No. 31870328) and Hubei Key Laboratory of Pollutant Analysis and Reuse Technology (No. PA160203).

Appendix A. Supplementary material

Supplementary data to this article can be found online at https://doi.org/10.1016/j.saa.2020.119297.

References

[1] R.K. Maheshwari, A.K. Singh, J. Gaddipati, R.C. Srimal, Multiple biological activities of curcumin: A short review, Biochem. Pharmacol. Life Sci. 78 (2006) 2081–2087.
[2] Y.-M. Song, J.-P. Xu, L. Ding, Q. Hou, J.-W. Liu, Z.-L. Zhu, Syntheses, characterization and biological activities of rare earth metal complexes with curcumin and 1,10-phenanthroline-5,6-dione, J. Inorg. Biochem. 103 (2009) 396–400.
[3] E. Ferrari, F. Pignedoli, C. Imbriano, G. Marverti, V. Basile, E. Venturi, M. Saladini, Newly Synthesized curcumin derivatives: crosstalk between chemico-physical properties and biological activity, J. Med. Chem. 54 (2011) 8066–8077.
[4] J. Lal, S.K. Gupta, D. Thavaselvam, D.D. Agarwal, Biological activity, design, synthesis and structure activity relationship of some novel derivatives of curcumin containing sulfonamides, Eur. J. Med. Chem. 64 (2013) 579–588.
[5] W. Liu, Y. Li, Y. Yue, K. Zhang, Q. Chen, H. Wang, Y. Lu, M.-T. Huang, X. Zheng, Z. Du, Synthesis and biological evaluation of curcumin derivatives containing NSAIDs for their anti-inflammatory activity, Bioorg. Med. Chem. Lett. 25 (2015) 3044–3051.
[6] K. Krishnankutty, P. Venugopalan, Metal chelates of curcuminoids, Synth. React. Inorg. Met.-Org. Chem. 28 (1998) 1313–1325.
[7] V.D. John, M.B. Ummathur, K. Krishnankutty, Synthesis, characterization, and antitumour studies of some curcuminoid analogues and their aluminum complexes, J. Coord. Chem. 66 (2013) 1508–1518.
[8] P. Li, W. Su, X. Lei, Q. Xiao, S. Huang, Synthesis, characterization and anticancer activity of a series of curcuminoids and their half-sandwich ruthenium(II) complexes, Appl. Organometal. Chem. 31 (2017) e3685.
[9] G. Began, E. Sudharshan, K.U. Sankar, A.G.A. Rao, Interaction of curcumin with phosphatidylcholine: a spectrofluorometric study, J. Agric. Food Chem. 47 (1999) 4992–4997.
[10] Z.G. Chen, L. Zhu, T.H. Song, J.H. Chen, Z.M. Guo, A novel curcumin assay with the metal ion Cu (II) as a simple probe by resonance light scattering technique, Spectrochim. Acta A 72 (2009) 518–522.
[11] K. Liu, T.L. Guo, J. Chojnacki, H.G. Lee, S.L. Siedlak, S.J. Zhang, Bivalent ligand containing curcumin and cholesterol as a fluorescence probe for Aβ plaques in Alzheimer's disease, ACS Chem. Neurosci. 3 (2012) 141–146.
[12] A. Felouat, A. D'Aléo, F. Fages, Synthesis and photophysical properties of difluoroboron complexes of curcuminoid derivatives bearing different terminal aromatic units and a meso-aryl ring, J. Org. Chem. 78 (2013) 4446–4455.
[13] G. Bai, C. Yu, C. Cheng, E. Hao, Y. Wei, X. Mu, L. Jiao, Syntheses and photophysical properties of BF_2 complexes of curcumin analogues, Org. Biomol. Chem. 12 (2014) 1618–1626.
[14] M. Rivoal, E. Zaborova, G. Canard, A. D'Aléo, F. Fages, Synthesis, electrochemical and photophysical studies of the borondifluoride complex of a meta-linked biscurcuminoid, New J. Chem. 40 (2016) 1297–1305.
[15] C. Ran, X. Xu, S.B. Raymond, B.J. Ferrara, K. Neal, B.J. Bacskai, Z. Medarova, A. Moore, Design, synthesis, and testing of difluoroboron-derivatized curcumins as near-infrared probes for in vivo detection of amyloid-β deposits, J. Am. Chem. Soc. 131 (2009) 15257–15261.
[16] A. Chaicham, S. Kulchat, G. Tumcharern, T. Tuntulani, B. Tomapatanaget, Synthesis, photophysical properties, and cyanide detection in aqueous solution of BF_2-curcumin dyes, Tetrahedron 66 (2010) 6217–6223.
[17] S.N. Margar, L. Rhyman, P. Ramasami, N. Sekar, Fluorescent difluoroboron-curcumin analogs: An investigation of the electronic structures and photophysical properties, Spectrochim. Acta Part A 152 (2016) 241–251.
[18] Z. Li, Y. Song, Z. Lu, Z. Li, R. Li, Y. Li, S. Hou, Y.-P. Zhu, H. Guo, Novel difluoroboron complexes of curcumin analogues as "dual-dual" sensing materials for volatile acid and amine vapors, Dyes Pigm. 179 (2020) 108406.
[19] H. Lyu, D. Wang, L. Cai, D.-J. Wang, X.-M. Li, Synthesis, photophysical and solvatochromic properties of diacetoxyboron complexes with curcumin derivatives, Spectrochim. Acta Part A 220 (2019) 117126.
[20] S.I. Klink, G.A. Hebbink, L. Grave, F.G.A. Peters, F.C.J.M. Van Veggel, D.N. Reinhoudt, J.W. Hofstraat, Near-infrared and visible luminescence from terphenyl-based lanthanide(III) complexes bearing amido and sulfonamido pendant arms, Eur. J. Org. Chem. 2000 (2000) 1923–1931.
[21] A. Beeby, I.M. Clarkson, R.S. Dickins, S. Faulkner, D. Parker, L. Royle, A.S. de Sousa, J.A.G. Williams, M. Woods, Nonradiative deactivation of the excited states of europium, terbium and ytterbium complexes by proximate energy-matched OH, NH and CH oscillators: an improved luminescence method for establishing solution hydration states, J. Chem. Soc. Perkin Trans. 2 (1999) 493–504.
[22] H.-D. Ilge, E. Birckner, D. Fassler, M.V. Kozmenko, M.G. Kuz'min, H. Hartmann, Spectroscopy, photophysics and photochemistry of 1,3-diketoboronates: IV: Luminescence spectroscopic investigations of 2-naphthyl-substituted 1,3-diketoboronates, J. Photochem. 32 (1986) 177–189.
[23] J.-L.M. Abboud, R. Notario, Critical compilation of scales of solvent parameters. Part I. Pure, non-hydrogen bond donor solvents, Pure Appl. Chem. 71 (1999) 645–718.
[24] C. Reichardt, Solvatochromic dyes as solvent polarity indicators, Chem. Rev. 94 (1994) 2319–2358.
[25] H. Liu, S. Yan, R. Huang, Z. Gao, G. Wang, L. Ding, Y. Fang, Single-benzene-based solvatochromic chromophores: color-tunable and bright fluorescence in the solid and solution states, Chem. Eur. J. 25 (2019) 16732–16739.
[26] A. Marini, A. Muñoz-Losa, A. Biancardi, B. Mennucci, What is solvatochromism, J. Phys. Chem. B 114 (2010) 17128–17135.
[27] U.P. Raghavendra, M. Basanagouda, R.M. Melavanki, R.H. Fattepur, J. Thipperudrappa, Solvatochromic studies of biologically active iodinated 4-aryloxymethyl coumarins and estimation of dipole moments, J. Mol. Liq. 202 (2015) 9–16.
[28] A.N. Kursunlu, Synthesis and photophysical properties of modifiable single, dual, and triple-boron dipyrromethene (Bodipy) complexes, Tetrahedron Lett. 56 (2015) 1873–1877.
[29] C. Qian, G. Hong, M. Liu, P. Xue, R. Lu, Star-shaped triphenylamine terminated difluoroboron β-diketonate complexes: synthesis, photophysical and electrochemical properties, Tetrahedron 70 (2014) 3935–3942.
[30] J.R. Lakowicz, Principles of Fluorescence Spectroscopy, third ed., Springer, New York, 2006.
[31] E. Bozkurta, H.I. Gulb, E. Mete, Solvent and substituent effect on the photophysical properties of pyrazoline derivatives: a spectroscopic study, J. Photochem. Photobiol. A 352 (2018) 35–42.
[32] P. Suppan, Excited-state dipole moments from absorption/fluorescence solvatochromicratios, Chem. Phys. Lett. 3 (1983) 272–275.
[33] B. Siddlingeshwar, S.M. Hanagodimath, Estimation of first excited singlet-state dipole moments of aminoanthraquinones by solvatochromic method, Spectrochim. Acta A 72 (2009) 490–495.
[34] Y.H. Pang, S.M. Shuang, M.S. Wong, Z.H. Li, C. Dong, Study on photophysical properties of intramolecular charge transfer (ICT) compound: 4-(diphenylamino) biphenyl-4'-boronic acid, J. Photochem. Photobiol. A 170 (2005) 15–19.
[35] K. Ono, K. Yoshikawa, Y. Tsuji, H. Yamaguchi, R. Uozumi, M. Tomura, et al., Synthesis and photoluminescence properties of BF_2 complexes with 1,3-diketone ligands, Tetrahedron 63 (2007) 9354–9358.
[36] H.-H. Zhang, X. Hu, W. Dou, W.-S. Liu, Photoluminescence properties of new BF_2 complexes with pyrazolone ligands: dependence on volume and electronic effect of substituents, J. Fluorine Chem. 131 (2010) 883–887.
[37] S. Song, J. Chen, W. Pan, H. Song, H. Shi, Y. Mai, W. Wen, LED based on alternating benzene-furan oligomers, Spectrochim. Acta A 170 (2017) 157–166.